

BRIEF REPORTS

*Brief Reports are accounts of completed research which, while meeting the usual **Physical Review B** standards of scientific quality, do not warrant regular articles. A Brief Report may be no longer than four printed pages and must be accompanied by an abstract. The same publication schedule as for regular articles is followed, and page proofs are sent to authors.*

Analytical expression for the optimized stop bands of fcc photonic crystals in the scalar-wave approximation

İ. Inanç Tarhan and George H. Watson

Department of Physics and Astronomy, University of Delaware, Newark, Delaware 19716

(Received 18 March 1996; revised manuscript received 14 June 1996)

We present an analytical model based on scalar-wave approximation to study the stop bands of face-centered-cubic photonic crystals with dielectric spheres at lattice sites. An analytical expression is obtained for the normalized stop band widths along the [111] and [100] directions as a function of volume fraction and relative dielectric contrast. These calculations enable us to map out the dielectric constants and volume fractions which results in *overlapping L and X* stop bands. From this map, it is possible to extract the optimum volume fraction that results in the widest overlapping stop band for a given dielectric contrast. We find that the relation between the optimum volume fraction and the dielectric contrast can be approximated by a simple power-law behavior for fcc photonic crystals. [S0163-1829(96)01036-3]

Photonic band gap (PBG) crystals belong to an interesting class of materials that are characterized by strong periodic modulations in the dielectric constant, preferably in all three dimensions. In such a crystal, propagation of electromagnetic waves is forbidden for a certain frequency range regardless of the incident direction of photons; thus spontaneous emission can be controlled, opening up the possibility of many device applications, especially in the optical regime.¹ The concept of three-dimensional photonic crystals was introduced by Yablonovitch² in 1987, and also independently by John³ in the context of photon localization.

Although most applications of PBG materials will be in the optical regime, fabrication of a three-dimensional photonic crystal with a complete PBG for this regime has not been possible yet. We recently reported experimental measurements of the optical-photonic band structure of three-dimensional photonic crystals, formed by polystyrene microspheres suspended in water arranged in a fcc lattice;^{4,5} however, an overall overlap in the stop bands along different directions was not achieved, owing to the low dielectric contrast $\epsilon_c = 1.43$. Although various computational tools such as vector-wave⁶⁻¹⁰ and transmission matrix method calculations¹¹⁻¹⁴ have been introduced to study the photonic band structure of two- or three-dimensional dielectric struc-

tures, there has been a shortage of simple and less time-consuming tools for investigating photonic crystals. To fill this gap, we have developed an analytical model for optimizing *optical stop bands* of fcc photonic crystals with a spherical basis based on scalar-wave approximation.¹⁵⁻¹⁷

The electric field in a photonic crystal, comprised of linear, lossless material, can be obtained from Maxwell's equations

$$-\nabla^2 \mathbf{E}(\mathbf{r}) - \frac{\omega^2}{c^2} \epsilon'(\mathbf{r}) \mathbf{E}(\mathbf{r}) = \epsilon_o \frac{\omega^2}{c^2} \mathbf{E}(\mathbf{r}), \quad (1)$$

where the dielectric constant is separated into two parts:

$$\epsilon(\mathbf{r}) = \epsilon'(\mathbf{r}) + \epsilon_o.$$

ϵ_o is the average and ϵ' is the fluctuating or periodic part of the dielectric constant. The average dielectric constant is taken as

$$\epsilon_o = f \epsilon_a + (1-f) \epsilon_b = [(\epsilon_c - 1)f + 1] \epsilon_b, \quad (2)$$

where f is the volume fraction of the dielectric spheres in the crystal, ϵ_a (ϵ_b) is the dielectric constant of the microspheres

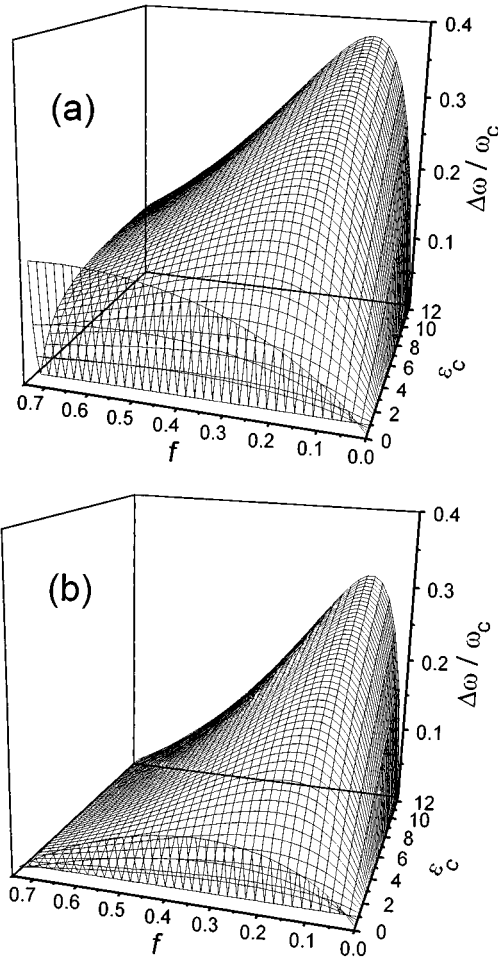


FIG. 1. Dependence of the normalized fcc symmetry direction stop bandwidths on the volume fraction and the dielectric contrast along (a) [111] L -point and (b) [100] X -point directions.

(background medium), and $\epsilon_c = \epsilon_a / \epsilon_b$ is the dielectric contrast. The volume fraction for a fcc crystal (four spherical atoms in one unit cell) is given as

$$f = 4 \frac{(4/3) \pi R_s^3}{a^3}, \quad (3)$$

where a is the lattice constant, and R_s is the radius of the atom. The periodic part of the dielectric constant of the photonic crystal, $\epsilon'(\mathbf{r})$, can be represented by the following equation:

$$\epsilon'(\mathbf{r}) = (\epsilon_c - 1) \epsilon_b \sum_{\mathbf{R}} \theta(R_s - |\mathbf{r} - \mathbf{R}|), \quad (4)$$

where $\theta(x)$ is the unit step function, where $\theta(x) = 1$ for $x \geq 0$ and zero otherwise;¹⁵ the summation is over all the dielectric spheres centered at \mathbf{R} with radius R_s . Also, $\epsilon'(\mathbf{r})$ can be expanded in the usual way as

$$\epsilon'(\mathbf{r}) = \sum_{\mathbf{G}} U_{\mathbf{G}} e^{i\mathbf{G} \cdot \mathbf{r}}, \quad (5)$$

where \mathbf{G} is a reciprocal-lattice vector. Thus the Fourier coefficients $U_{\mathbf{G}}$ are given by

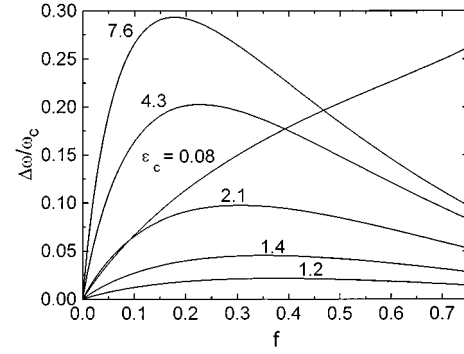


FIG. 2. Dependence of the normalized fcc [111] stop bands on the volume fraction. Note that as $\epsilon_c \rightarrow 1$, the stop band width stays almost constant for most values of the volume fraction.

$$U_{\mathbf{G}} = \frac{1}{\Omega} \int (\epsilon_c - 1) \epsilon_b \sum_{\mathbf{R}} \theta(R_s - |\mathbf{r} - \mathbf{R}|) e^{-i\mathbf{G} \cdot \mathbf{r}} d^3r, \quad (6)$$

where Ω is the volume of the primitive unit cell of the crystal. From Eq. (6), the Fourier coefficients for a fcc lattice with spherical ‘atoms’ are found as

$$U_{\mathbf{G}} = -\frac{16\pi}{(aG)^3} (\epsilon_c - 1) \epsilon_b [\sin(GR_s) - GR_s \cos(GR_s)]. \quad (7)$$

The electric field $\mathbf{E}(\mathbf{r})$ is treated here as scalar, and expanded into Bloch states

$$E(\mathbf{r}) = \sum_{\mathbf{G}} \sum_{\mathbf{k}} C_{\mathbf{k}-\mathbf{G}} e^{i(\mathbf{k}-\mathbf{G}) \cdot \mathbf{r}}, \quad (8)$$

where $\sum_{\mathbf{k}}$ is summed over the first Brillouin zone. Near the L point ($k = G_L/2$), Bloch scattering due to U_{G_L} dominates (similarly U_{G_X} for the X point), thus the scalar-wave approximation in Eq. (8) is reasonable. By rewriting Eq. (1), and approximating $G = G_{L(X)}$ for bands near $L(X)$ the photonic dispersion relation $k(\omega)$ can be obtained in the following form:¹⁸

$$k = G/2 \pm \sqrt{F(\omega)}, \quad (9)$$

where

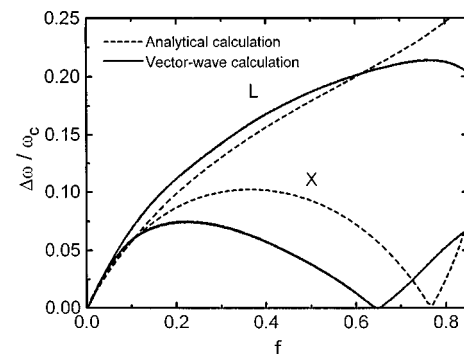


FIG. 3. Comparison of the analytical model (dashed) with the vector-wave calculations (solid) taken from Ref. 16. The gap widths are normalized by the central frequency of the X -point gap.

$$F(\omega) = (G^2/4) + \epsilon_o(\omega^2/c^2) - \sqrt{G^2\epsilon_o(\omega^2/c^2) + U_G^2(\omega^4/c^4)}. \quad (10)$$

Positive $F(\omega)$ corresponds to band modes where k is real, and negative $F(\omega)$ to gap modes where k is complex. For gap modes,

$$k = G/2 \pm iq,$$

where $q = \sqrt{|F(\omega)|}$. Note that the imaginary part of the wave vector exists only for the modes which are in the band gap. These gap modes exist only at the surface or interfaces; otherwise the amplitude of the field would grow exponentially, an unphysical situation.¹⁸ It is possible to find the frequencies for which $F(\omega) = 0$, and thus the boundaries of the frequency window in which the gap modes exist:

$$\omega_{\pm} = \frac{1}{2} \frac{cG}{\sqrt{\epsilon_o \pm U_G}}. \quad (11)$$

We define the width of the photonic stop band as $\Delta\omega = |\omega_- - \omega_+|$, and the gap center frequency as $\omega_c = (\omega_- + \omega_+)/2$ such that the normalized stop band width $\Delta\omega/\omega_c$ is given as

$$\frac{\Delta\omega}{\omega_c} = 2 \frac{|\omega_- - \omega_+|}{\omega_- + \omega_+} = 2 \left| \frac{U_G}{\epsilon_o + \sqrt{\epsilon_o^2 - U_G^2}} \right|. \quad (12)$$

To calculate the normalized stop band width for fcc symmetry directions, the reciprocal-lattice vector is taken as $G = 2\pi\alpha/a$, where $\alpha = \sqrt{3}$ ($\alpha = 2$) is used for $\Gamma \rightarrow L$ ($\Gamma \rightarrow X$) stop bands. Equation (7) can be written as

$$U_G = -\frac{2}{\alpha^3 \pi^2} (\delta\epsilon_c) \epsilon_b (\sin\xi - \xi \cos\xi), \quad (13)$$

where $\xi^3 = 3\alpha^3 \pi^2 f/2$ and $\delta\epsilon_c = \epsilon_c - 1$. Thus the normalized stop band is calculated as

$$\frac{\Delta\omega}{\omega_c} = \left| \frac{4\delta\epsilon_c(\sin\xi - \xi \cos\xi)}{\pi^2 \alpha^3 (f\delta\epsilon_c + 1) + \sqrt{\alpha^6 \pi^4 (f\delta\epsilon_c + 1)^2 - 4\delta\epsilon_c^2 (\sin\xi - \xi \cos\xi)^2}} \right|. \quad (14)$$

Note that Eq. (14) depends only on the relative dielectric contrast ϵ_c and volume fraction f (through ξ). Since the close-packed volume fraction for fcc is 0.74, Eq. (14) is expected to be valid for $f \leq 0.74$. For $f > 0.74$, the atoms start to overlap, and become connected losing their spherical shape.

In Figs. 1(a) and 1(b), Eq. (14) is plotted for the L and X stop bands, respectively. Note that for both cases, as $\epsilon_c \rightarrow 1$, the stop band vanishes as expected. Also, in Fig. 1(b), the stop band along the X -point direction approaches zero as, $f \rightarrow 0.7$ as discussed in Ref. 19. At this volume fraction, the Fourier coefficient of the dielectric modulation U_G changes sign due to a shift of material density from the interstitial layers to the cube faces. From Eq. (13), this occurs at $f = 0.77$, when $\tan\xi = \xi$ thus it is independent of ϵ_c .

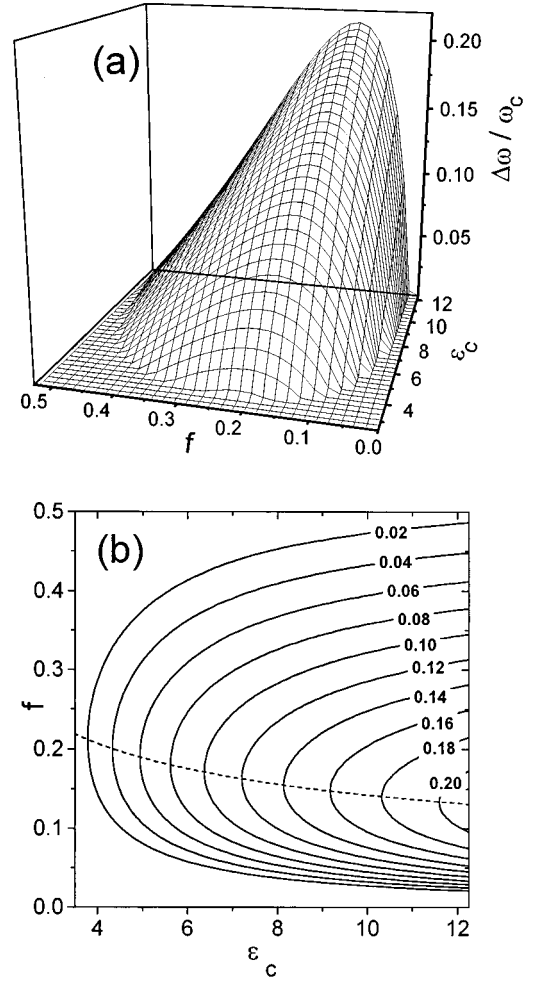


FIG. 4. Region of overlap for X and L stop bands. The center frequency ω_c is the frequency at the center of the overlapping bands. (a) Surface plot. (b) Contour plot in the $f - \epsilon_c$ plane. The dashed line is the optimum volume fraction, f_{LX-opt} for the widest stop band. Values of $\Delta\omega/\omega_c$ are labeled.

Several cross sections in the $f - (\Delta\omega/\omega_c)$ plane of Fig. 1(a) taken at particular dielectric contrast values are shown in Fig. 2. The interesting feature here is the location of the maximum stop band width. Note that as the dielectric contrast increases ($\epsilon_c > 1$), f_{L-opt} shifts to lower values ($f \sim 10-20\%$). For $\epsilon_c < 1$, this trend reverses, and for $\epsilon_c \ll 1$, f_{L-opt} exceeds the close packed limit.

In Fig. 3, we compare our analytical results with the vector-wave calculations of Leung and Liu.¹⁶ The photonic crystals modeled in Ref. 16 were experimentally realized by Yablonovitch and Gmitter¹⁹ by drilling air holes in a host medium with $\epsilon_b = 12.25$ ($\epsilon_c = 0.082$). The L -point stop bands show fairly good agreement with the full vector-wave calculation, whereas X -point stop bands display only qualitative agreement. Specifically, the X -point stop band goes to

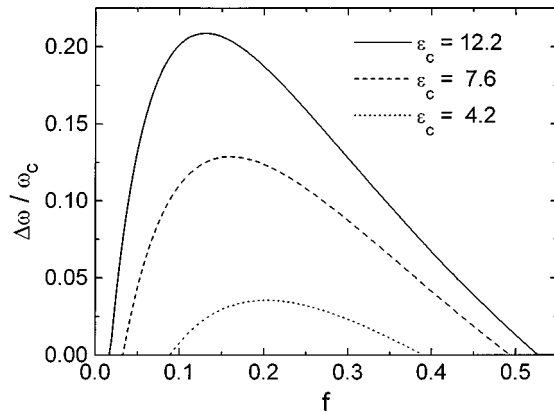


FIG. 5. Dependence of the normalized overlap of the X and L stop bands on the volume fraction.

zero for $f=0.66$ (for $\epsilon_c=0.082$) in the vector-wave calculation, in good agreement with $f=0.68$ with the experiment of Yablonovitch and Gmitter, whereas the analytical case predicts $f=0.77$ (for $0.08 < \epsilon_c < 12.5$). The discrepancy here might result from the breakdown of the scalar-wave approximation and the basic assumption of the Bloch scattering being dominated by only one U_G in this regime where $\epsilon_c \ll 1$ as well as for $\epsilon_c \gg 1$. The sample studied in Ref. 5, polystyrene microspheres in water with $f=0.05$ ($\epsilon_c=1.43$) yielded a normalized experimental gap of 0.0152 at the L point,²⁰ which is in excellent agreement with a calculated gap of 0.0159 from Eq. (14).

It is also possible to calculate the region in the $f-\epsilon_c$ plane that results in *overlapping* L and X stop bands. This can be obtained by using Eq. (11) for L and X bands. In Fig. 4, the overlapping region is shown for $\epsilon_c > 1$. For $\epsilon_c < 1$, the overlapping region occurs for volume fractions that exceed the close-packing limit, and thus it is not displayed. The optimum volume fraction for maximum L - and X -band overlap is shown in Fig. 4(b) as the line crossing the constant normalized gap contours.

Several cross sections in the $f-(\Delta\omega/\omega_c)$ plane of Fig. 4(a) taken at particular dielectric contrast values are seen in Fig. 5. The interesting feature here is the location of the maximum stop band width. Note that as the dielectric contrast increases ($\epsilon_c > 1$), f_{LX-opt} shifts to lower values.

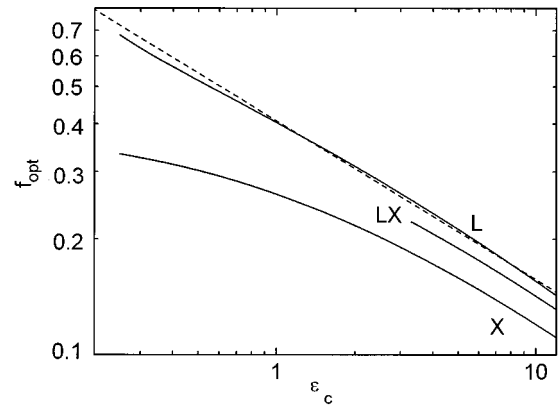


FIG. 6. Numerical solution for f_{opt} as a function of the dielectric contrast. The power-law fit to f_{L-opt} is shown with the dashed line. The power-law fit to f_{LX-opt} is not shown, for clarity.

In Fig. 6, the optimum volume fraction for the L , X , and overlapping bands are plotted in the same log-log graph. The optimum volume fraction for the L band [Fig. 3(a)] can be approximated reasonably well by a power-law behavior $\beta\epsilon_c^{-\gamma}$ for two decades of dielectric contrast. From the parameters of the linear fit to the f_{L-opt} curve, we find $\beta=0.41$ and $\gamma=0.41$. Similarly, the optimum volume fraction for overlapping X and L bands shown in Fig. 4(a) can be approximated well by the power-law behavior, but with a coefficient $\beta=0.36$ for $3 < \epsilon_c < 12.5$.

In conclusion, we have presented an analytical model using the *scalar-wave approximation* for calculating the stop band widths of fcc photonic crystals with a spherical basis. Although vector-wave calculations more accurately determine details of the photonic band structure, our scalar-wave model is useful in predicting optimal conditions for band overlap for this specific case. This model can be used for calculating the characteristics of stop bands along the fcc close-packing and cubic directions. From this expression, it is possible to obtain the parameters that result in overlapping L and X bands. We have found a power-law type relation which can be used as a guide in the optimization of such crystals.

This work was supported by the National Science Foundation under Grant No. DMR95-10460.

¹For a recent review, see *Photonic Band Gap Materials*, edited by C. M. Soukoulis (Kluwer Academic, Dordrecht, 1996).

²E. Yablonovitch, Phys. Rev. Lett. **58**, 2059 (1987).

³S. John, Phys. Rev. Lett. **58**, 2486 (1987).

⁴İ. İ. Tarhan, M. P. Zinkin, and G. H. Watson, Opt. Lett. **20**, 1571 (1995).

⁵İ. İ. Tarhan and G. H. Watson, Phys. Rev. Lett. **76**, 315 (1996).

⁶K. M. Leung and Y. F. Liu, Phys. Rev. Lett. **65**, 2646 (1990).

⁷Z. Zhang and S. Satpathy, Phys. Rev. Lett. **65**, 2650 (1990).

⁸K. M. Ho, C. T. Chan, and C. M. Soukoulis, Phys. Rev. Lett. **65**, 3152 (1990).

⁹H. S. Sözüer, J. W. Haus, and R. Inguva, Phys. Rev. B **45**, 13 962 (1992).

¹⁰R. D. Meade, A. M. Rappe, K. D. Brommer, J. D. Joannopoulos, and O. L. Alerhand, Phys. Rev. B **48**, 8434 (1993).

¹¹J. B. Pendry and A. MacKinnon, Phys. Rev. Lett. **69**, 2772 (1992).

¹²M. Sigalas, C. M. Soukoulis, E. N. Economou, C. T. Chan, and K. M. Ho, Phys. Rev. B **48**, 14 121 (1993).

¹³J. B. Pendry, J. Mod. Opt. **41**, 209 (1994).

¹⁴P. M. Bell *et al.*, Comput. Phys. Commun. **85**, 306 (1995).

¹⁵S. Satpathy, Z. Zhang, and M. R. Salehpour, Phys. Rev. Lett. **64**, 1239 (1990).

¹⁶K. M. Leung and Y. F. Liu, Phys. Rev. B **41**, 10 188 (1990).

¹⁷S. Datta, C. T. Chan, K. M. Ho, and C. M. Soukoulis, Phys. Rev. B **46**, 10 650 (1992).

¹⁸K. W.-K. Shung and Y. C. Tsai, Phys. Rev. B **48**, 11 265 (1993).

¹⁹E. Yablonovitch and T. J. Gmitter, Phys. Rev. Lett. **63**, 2269 (1988).

²⁰There is always some arbitrariness in extracting the width of the

optical stop bands from experimental transmission measurements of photonic crystals with a finite thickness. In our recent experiments, the bandwidth was extracted as the full width at two orders of magnitude below unity transmission.